Observations of Extrasolar Planets During the non-Cryogenic Spitzer Space Telescope Mission

Drake Deming[*], Eric Agol[†], David Charbonneau[**], Nicolas Cowan[†], Heather Knutson[**] and Massimo Marengo[‡]

[*]*NASA's Goddard Space Flight Center, Planetary Systems Laboratory, Code 693, Greenbelt, MD 20771, USA*
[†]*Department of Astronomy, University of Washington, Box 351580, Seattle, WA 98195-1580, USA*
[**]*Department of Astronomy, Harvard University, 60 Garden St., MS-16, Cambridge, MA 02138, USA*
[‡]*Harvard-Smithsonian Center for Astrophysics, 60 Garden St., MS-45, Cambridge, MA 02138, USA*

Abstract. Precision infrared photometry from Spitzer has enabled the first direct studies of light from extrasolar planets, via observations at secondary eclipse in transiting systems. Current Spitzer results include the first longitudinal temperature map of an extrasolar planet, and the first spectra of their atmospheres. Spitzer has also measured a temperature and precise radius for the first transiting Neptune-sized exoplanet, and is beginning to make precise transit timing measurements to infer the existence of unseen low mass planets. The lack of stellar limb darkening in the infrared facilitates precise radius and transit timing measurements of transiting planets. Warm Spitzer will be capable of a precise radius measurement for Earth-sized planets transiting nearby M-dwarfs, thereby constraining their bulk composition. It will continue to measure thermal emission at secondary eclipse for transiting hot Jupiters, and be able to distinguish between planets having broad band emission *vs.* absorption spectra. It will also be able to measure the orbital phase variation of thermal emission for close-in planets, even non-transiting planets, and these measurements will be of special interest for planets in eccentric orbits. Warm Spitzer will be a significant complement to Kepler, particularly as regards transit timing in the Kepler field. In addition to studying close-in planets, Warm Spitzer will have significant application in sensitive imaging searches for young planets at relatively large angular separations from their parent stars.

Keywords: Spitzer Space Telescope, infrared astronomical observations, extrasolar planets
PACS: 95.85.Hp, 97.82.Cp, 97.82.Jw, 97.82.Fs

1. INTRODUCTION

The Spitzer Space Telescope (Werner *et al.* [1]) was the first facility to detect photons from known extrasolar planets (Charbonneau *et al.* [2], Deming *et al.* [3]), inaugurating the current era wherein planets orbiting other stars are being studied directly. Cryogenic Spitzer has been a powerful facility for exoplanet characterization, using all three of its instruments. Spitzer studies have produced the first temperature map of an extrasolar planet (Knutson *et al.* [4]), and the first spectra of their atmospheres (Grillmair *et al.* [5], Richardson *et al.* [6]). Spitzer will continue to study exoplanets when its store of cryogen is exhausted. 'Warm Spitzer' (commencing $\sim$ spring 2009) will remain at T $\sim$ 35K (passively cooled by radiation), allowing imaging photometry at 3.6 and 4.5 μm, at full sensitivity. The long observing times that are projected for the warm mission will facilitate several pioneering exoplanet studies not contemplated for the cryogenic

mission.

2. EXTRASOLAR PLANETS IN 2009

Currently over 200 extrasolar planets are known, including 22 transiting planets (17 orbiting stars brighter than V=13). Some of these have been discovered by the Doppler surveys, but an increasing majority of the transiting systems are being discovered by ground-based photometric surveys. However, the Doppler surveys remain an efficient method to find hot Jupiters, and surveys such as N2K (Fischer *et al.* [7]) continue to be a productive source of both transiting and non-transiting close-in exoplanets. The discovery rate from the photometric surveys is accelerating, because these teams have learned to efficiently identify and cull their transiting candidates, and quickly eliminate false positives. Several transit surveys (HAT, TrES, and XO) recently announced multiple new giant transiting systems (Burke *et al.* [8], O'Donovan *et al.* [9], Johns-Krull *et al.* [10], Mandushev *et al.* [11], Torres *et al.* [12]), and a Neptune-sized planet has been discovered transiting the M-dwarf GJ 436 (Gillon *et al.* [13]). We estimate that the number of bright (V<13) stars hosting transiting giant planets will increase to ∼100 in the Warm Spitzer time frame.

The discovery of transits in GJ 436b has stimulated interest in finding more M-dwarf planets, both by Doppler surveys (Butler *et al.* [14]), and using new transit surveys targeted at bright M-dwarfs. It is reasonable to expect that ∼10 transiting hot Neptunes will be discovered transiting bright M-dwarf stars by the advent of the warm mission. Moreover, the Doppler surveys are finding planets orbiting evolved stars (Johnson *et al.* [15]). The greater luminosity of evolved stars can potentially super-heat their close-in planets and facilitate follow-up by Warm Spitzer at 3.6 and 4.5 μm.

3. PHOTOMETRY USING WARM SPITZER

Warm Spitzer has a particularly important role in follow up for bright transiting exoplanet systems, as well as non-transiting systems, because in 2009 it will be the largest aperture general-purpose telescope in heliocentric orbit. Heliocentric orbit provides a thermally stable environment, and it allows long periods of observation, not blocked by the Earth. Although Kepler will have a greater aperture than Spitzer, Kepler will be locked-in to a specific field in Cygnus, so it cannot follow-up on the numerous bright transiting systems that will be discovered across the sky.

The thermally stable environment of heliocentric orbit has proven to be a boon for precision photometry from Spitzer. For example, the recent Spitzer 8 μm observations of the HD 189733b transit reported by Knutson *et al.* [4], illustrated in Fig. 1, are among the most precise transit observations ever made. These investigators measured the planet-to-star radius ratio for HD 189733b as 0.1545 ± 0.0002, corresponding to a precision of $\pm$ 90 km in the radius of the giant planet, and they also measured the orbital phase variation of the planet's thermal emission.
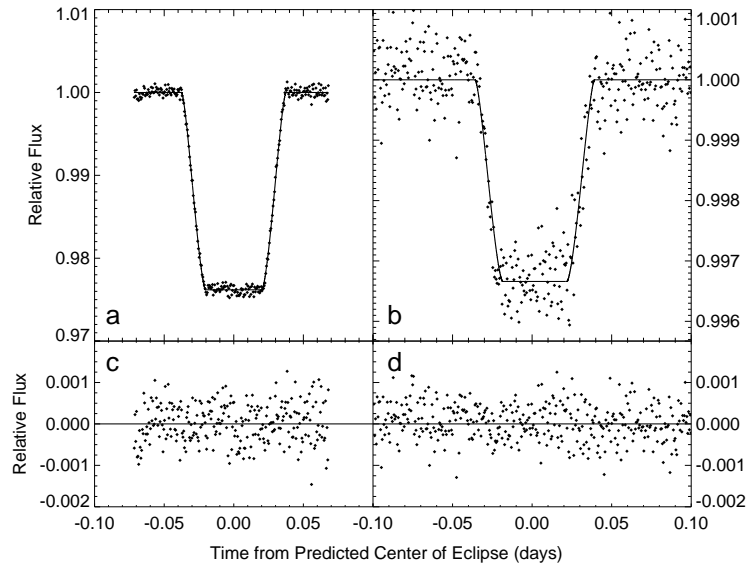
FIGURE 1. Transit (left) and a 60σ secondary eclipse detection (right) of HD 189733b at 8 μm using a continuous 33-hour Spitzer photometry sequence (Knutson *et al.* [4]).

4. MASS-RADIUS RELATIONS

Spitzer's precision for transits derives not only from its stable thermal environment, but also from the lack of stellar limb darkening in the IR. Without limb darkening, the transit becomes extremely 'box-like', with a flat bottom (Richardson *et al.* [16], Knutson *et al.* [4], see Fig. 1). The IR transit depth yields the ratio of planet to stellar area simply and directly, without the added uncertainty of fitting to limb-darkening. Spitzer is now the facility of choice for transiting planet radius measurements. A Warm Spitzer transit program - exploiting the bright stellar flux at 3.6 and 4.5 μm - could significantly improve our knowledge of the mass-radius relationship, and clarify differences in bulk composition, for all but the faintest hot Jupiter systems. Figure 2 shows the mass-radius relation for several of the transiting giant planets (Charbonneau *et al.* [17]). The mass-radius relation encodes fundamental information on the global structure of these planets. For example, HD 149026b is inferred to have a heavy element core of at least 70 Earth masses, based on the small radius for its mass (Fig. 2, and Sato *et al.* [18]). This information is crucial to our understanding of planet formation, e.g., by the core accretion and gravitational instability mechanisms (Lissauer & Stevenson [19]). The scientific utility of these measurements will be maximized if all transiting exoplanet radii are measured to high precision, in a mutually consistent manner. Moreover, as the Doppler and transit surveys discover Neptune to Earth-sized planets orbiting M-dwarfs, the highest precision photometry will be needed to measure their radii to a precision sufficient to constrain their interior structure.
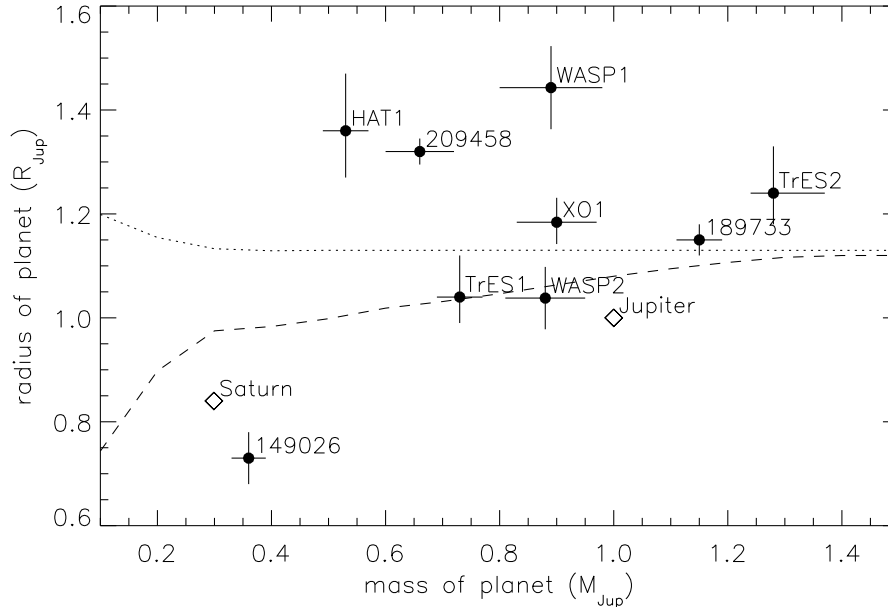
FIGURE 2. Mass-radius relation for giant transiting exoplanets, compared to Jupiter and Saturn (Charbonneau *et al.* [17]). The lines show the theoretical relations (Bodenheimer *et al.* [20] for planets having no core (dotted) and a 20 Earth-mass solid core (dashed).

4.1. Spitzer vs. Ground-Based Photometry

Ground-based photometry in the z-band is achieving sub-milli-magnitude levels of precision in many cases (Winn *et al.* [21]), and can determine the radii of some transiting giant planets to error limits imposed by astrophysical uncertainty in the stellar mass. The most favorable systems for ground-based observation are those occurring in fields with numerous nearby reference stars of comparable brightness. Planets transiting bright, spatially isolated, stars are not as favorable for ground observation. Moreover, as the radius of the transiting planet decreases, greater photometric precision is needed to reach the limits imposed by uncertainty in the stellar mass. Nearby M-dwarfs have flux peaks longward of the visible and z-band spectral regions, and they often lack nearby comparison stars of comparable infrared brightness. Neptune- to Earth-sized planets orbiting nearby M-dwarfs will therefore require infrared space-borne photometry for the best possible radius precision. Figure 3 illustrates a single transit of a 1-Earth radius planet across an M-dwarf, observed by Spitzer at 8 μm. We simulated this case by re-scaling a real case: Spitzer's recent photometry of GJ 436b (Deming *et al.* [22], Gillon *et al.* [23]). Spitzer's nearly photon-limited precision detects this Earth-sized planet to 7σ significance in a single transit.

Although Fig. 3 is based on Spitzer observations at 8 μm, the photon-limit for observations during the warm mission (e.g., at 4.5 μm) will be even more favorable, simply because stars are brighter at the shorter wavelength. Stellar photometry at the wavelengths used by the warm mission is affected by a pixel phase effect in the IRAC instru-
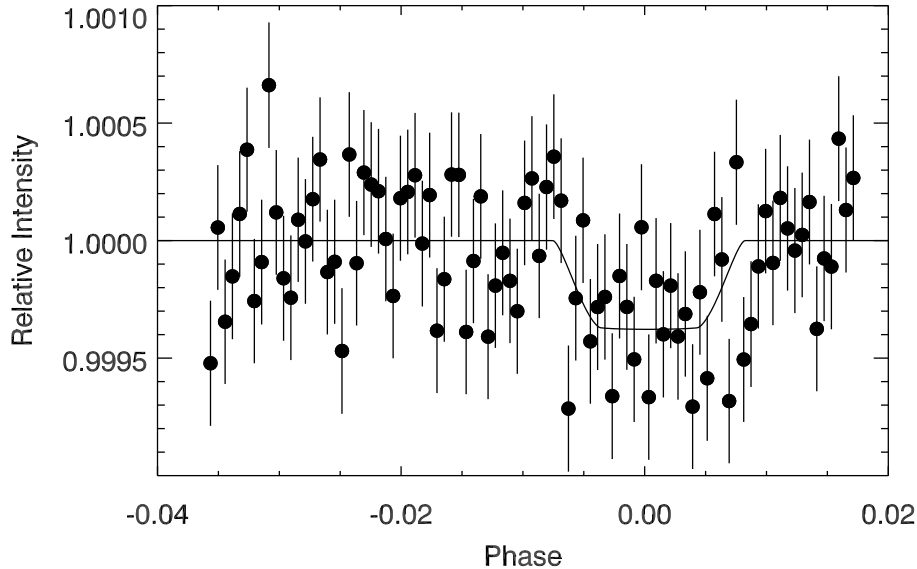
FIGURE 3. A transit of a 1 Earth radius planet across an M-dwarf, simulated by rescaling Spitzer 8 μm observations of GJ 436b (Deming *et al.* [22])

ment (Reach *et al.* [24]), but that can be successfully corrected by decorrelation (Charbonneau *et al.* [2]), and recent results have demonstrated secondary eclipse detections with a precision of $\sim 10^{-4}$ (Charbonneau *et al.* [2], Knutson *et al.* [25]). The pixel phase effect should be correctable to even greater precison using the large data sets contemplated for the warm mission.

5. NEW TYPES OF TRANSITING PLANETS

Ongoing Doppler and transit monitoring of known hot Jupiters can detect subtle deviations from Keplerian orbits (Charbonneau *et al.* [26]), indicating the presence of additional planets, e.g., 'warm Jupiters' in longer period orbits, or terrestrial mass planets in low order mean motion resonances. The likely co-alignment of orbital planes increases the chance those planets will also transit, and intensive radial velocity monitoring could constrain the transit time for giant planets. Warm Spitzer will be a sensitive facility for confirming those transits, and extending the mass-radius relation (Fig. 2) to planets in more distant orbits, and even to close-in terrestrial planets. Even lacking specific indications from Doppler measurements, searches for close-in terrestrial planets in low order mean motion resonances with known giant transiting planets (Thommes [27]) are warranted using Warm Spitzer. These searches could be combined with radius and transit timing measurements for the giant planets, in the same observing program.

For stars not known to host a hot Jupiter, ongoing Doppler surveys and space-borne transit surveys (e.g., COROT) will find more transiting planets, extending to Neptune
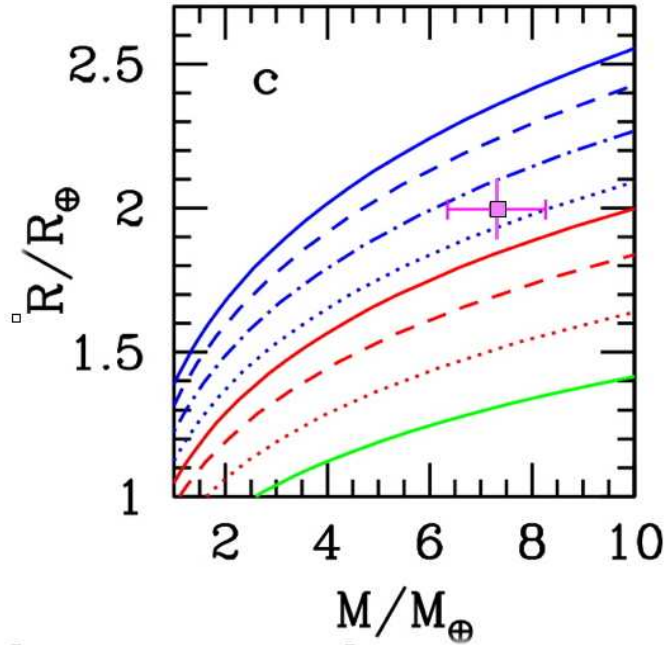
FIGURE 4. Mass-radius relations for solid exoplanets of various compositions, from Seager *et al.* [28]. Blue represents water ice planets, red are silicate planets, and green is a pure iron planet. The magenta point is a hypothetical observation of a hot Earth transiting an M-dwarf at 50 pc, observed by Warm Spitzer at 4.5 μm. The horizontal error bar is the mass error from Gliese 876d (Rivera *et al.* [29]); the vertical (radius) error bar is calculated for Warm Spitzer, not including error in the stellar radius.

mass and below. Spitzer transit measurements can precisely determine the radii of small planets. Exoplanet radius measurements and transit searches are particularly appropriate for Warm Spitzer, because: a) stars are bright in the 3.6 and 4.5 μm bands, while limb darkening is still absent, b) stellar activity is muted at IR wavelengths, and c) longer observing times are congruent with the goal of simplified operations in the extended mission. Figure 4 shows a potential example of a precise radius (allowing precise density) determination for a hot super-Earth, compared to the mass-radius relation for solid exoplanets of various composition (Seager *et al.* [28]). In this case, the Spitzer radius is sufficiently precise ($\pm$ 0.1 Earth radii) to constrain the bulk composition of this solid exoplanet by comparison to the Seager *et al.* [28] models.

6. THERMAL EMISSION AT 3.6 AND 4.5 μm

6.1. Absorption vs. Emission Spectra

The secondary eclipse of a transiting planet has the greatest depth at Spitzer's longest wavelengths. However, the eclipses are quite detectable at Spitzer's shortest wavelengths, because these are close to the peak of the Planck function at the temperatures of transiting planets. Secondary eclipse photometry using Warm Spitzer can therefore con-

tinue to define the brightness of exoplanets at 3.6 and 4.5 μm for new bright transiting systems. This will be especially valuable if complemented by ground-based detections exactly at the expected spectral peaks at 2.2 and 3.8 μm, which is believed to be feasible (Snellen and Covino [30], Deming *et al.* [31]). The predicted spectrum of a hot Jupiter exoplanet is illustrated in Fig. 5, from Charbonneau *et al.* [2]. Normally, the broad band spectrum is expected to be shaped by water vapor absorption. However, recent Spitzer photometry of HD 209458b (Knutson *et al.* [25]) indicates much better agreement with a spectrum wherein the water bands appear in *emission*, and can only be explained by the presence of a thermal inversion at high altitude (Burrows *et al.* [32]). The nature of the high altitude absorber needed to create this inversion is unknown, and may be connected to the specific properties of the system, such as the planet's level of irradiation or surface gravity. A comprehensive survey of the bright transiting systems would make it possible to search for correlations between the presence of a temperature inversion and other properties of the systems, thus providing insight into the origin of the inversions. Such a survey would also identify the best systems for spectroscopic follow up by JWST.

The signature of such an inversion is easily observed in the 3.6 and 4.5 μm Spitzer bandpasses. Standard models for atmospheres without temperature inversions predict that the planets will appear brighter at 3.6 μm than at 4.5 μm (see Fig. 5) due to the presence of water absorption bands at wavelengths longer than 4.5 μm. With a thermal inversion the relative brightnesses in the two bands are reversed, as the 3.6 μm flux is suppressed and the 4.5 μm flux is correspondingly enhanced by the presence of water emission at the longer wavelengths.

6.2. Temporal Variations Due to Dynamics

The cycle of variable stellar heating caused by planetary rotation can drive a lively dynamics in hot Jupiter atmospheres (Cooper & Showman [33]). In turn, the atmospheric dynamics will produce a spatially and temporally varing temperature field, and the temperature fluctuations are expected to be of large spatial scale for close-in planets (Rauscher *et al.* [34]). For the temperatures found in hot Jupiter atmospheres (T~1200K), the Planck function at Warm Spitzer wavelengths varies strongly with temperature. Consequently, temporal variations in thermal emission from close-in planets should be readily observable during the warm mission. The secondary eclipse depth of a given transiting system can vary, and observations of multiple eclipses could yield key insights into the atmospheric physics. Observations extended over a full orbit - even for non-transiting systems - can potentially reveal variations in thermal emission correlated with orbit phase (Cowan, Agol and Charbonneau [35]). Orbital phase variations can reflect the changing viewing geometry, but can also be caused by strong atmospheric dynamics in response to the variable stellar forcing that is characteristic of eccentric orbits.

Extrasolar planets have more eccentric orbits on average than do the planets of our own solar system. In some cases, their eccentricity extends to strikingly high values. For example, HD 80606b has an eccentricity of 0.93 (Naef *et al.* [36]). During its close periastron passage, it receives a stellar flux more than 1000 times greater than
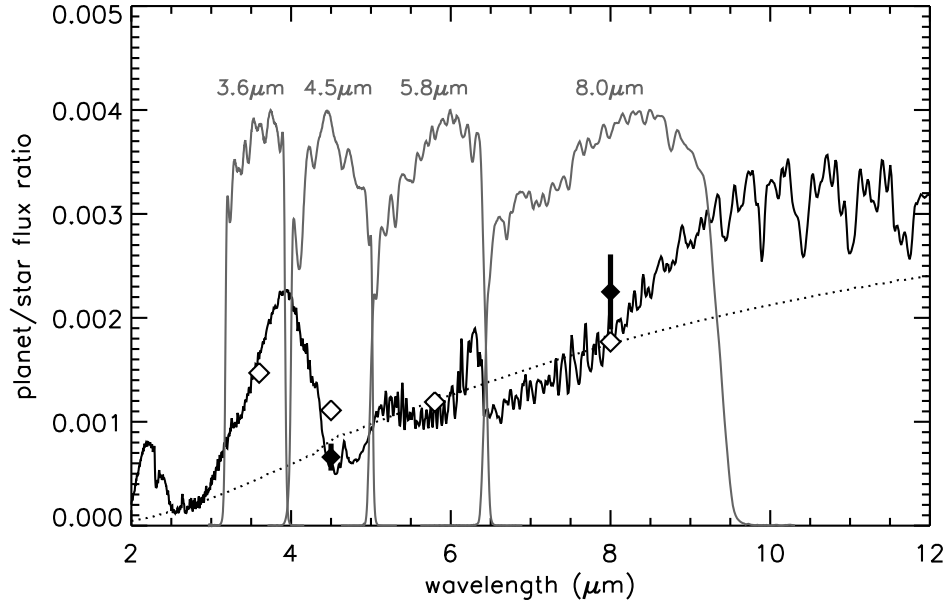
FIGURE 5. Predicted specturm of a hot Jupiter exoplanet, shown in comparison to observations of TrES-1 by Charbonneau *et al.* [2] (solid diamonds). The expected contrast (planet divided by star) for the IRAC bands is shown by open diamonds. Note the higher contrast expected at 3.6 μm compared to 4.5 μm, indicative of a water absorption spectrum. These contrast values will be reversed for a water emission spectrum. The dotted line is a blackbody spectrum.

the flux received by Earth from the Sun. This strong flux will cause a rapid heating of the planet's atmosphere, and its time dependence encodes crucial information on the radiative time scale, and thus the composition, of the planet's atmosphere (Langton and Laughlin [37]). This rapid heating of HD 80606b and similar systems may be observable at 3.6 and 4.5 μm. In this regard it is interesting to note that the exoplanet HD 185269b orbits a sub-giant star, having greater than solar luminosity, in a close orbit (6.8 day period), with an eccentricity of 0.3 (Johnson *et al.* [38]). The resultant strong variation in stellar heating over the orbit will force a corresponding variation in the planet's thermal emission, that should correlate with orbital phase. Recently, the transiting planets XO-3 and HAT-P-3 have also been found to have a significant eccentricity (Johns-Krull *et al.* [10], Torres *et al.* [12]), opening the possibility to also measure the spatial distribution of time dependent heating on the planet's disk (Williams *et al.* [39], Knutson *et al.* [4]). Given the high precision possible from Spitzer, it may be possible to observe all of these effects at 4.5 μm using Warm Spitzer.

7. TRANSIT TIMING

There is considerable recent interest in the indirect detection of extrasolar terrestrial planets via their perturbations to the transit times of giant transiting planets (Agol *et al.* [40], Holman and Murray [41], Steffen and Agol [42], Agol and Steffen [43]). Spitzer
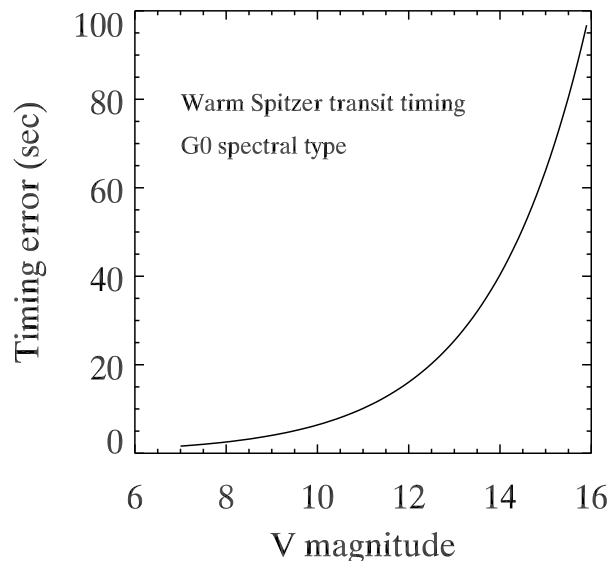
FIGURE 6. Calculation of the transit timing error (1σ) for Warm Spitzer observing giant planet transits at 4.5 μm, as a function of stellar brightness.

transit photometry during the warm mission is an excellent way to make precise transit timing measurements. The lack of IR limb darkening is again a significant advantage, because it results in very steep ingress and egress curves, producing excellent timing precision. Knutson *et al.* [4] found a timing precision for the HD 189733b transit of 6 seconds. Hubble transit timing errors range from 10 to 50 seconds (Agol and Steffen [43]), although a 3 second timing precision was recently achieved for HD 189733b by Pont *et al.* [44]. However, Spitzer has the advantage that the lower contrast of star spots and plage in the IR as compared to visible wavelengths minimizes systematic errors due to stellar activity noise. Also, Spitzer's heliocentric orbit permits continuous measurements before, during, and after transit - unlike Hubble where blocking by Earth interrupts transits. Moreover, Spitzer transit timing precision should be even better at the shorter wavelengths available for the warm mission, because stars are brighter at shorter wavelengths, and limb darkening remains negligible.

The continued success of the ground-based transit surveys, the advent of COROT, and the upcoming launch of Kepler, will provide a wealth of targets for Warm Spitzer follow-up. We have calculated the transit timing precision by Warm Spitzer at 3.6 and 4.5 μm, for solar-type stars at different distances (Fig. 6). This calculation is consistent with the Knutson *et al.* [4] result, and it projects a Spitzer timing precision of better than 40 seconds down to the faint end of Kepler's range at V=14. This is sufficient to detect perturbations by terrestrial planets well below one Earth mass in resonant orbits (Agol et al. 2005), or to $\sim 10\,(150\,\text{days}/P_1)$ Earth masses for $P_2/P_1 < 4$, where $P_{1,2}$ are the periods of the transiting and perturbing planets (Holman and Murray [41], Agol *et al.* [40]). The Warm Spitzer mission will begin at about the same time that Kepler begins to discover
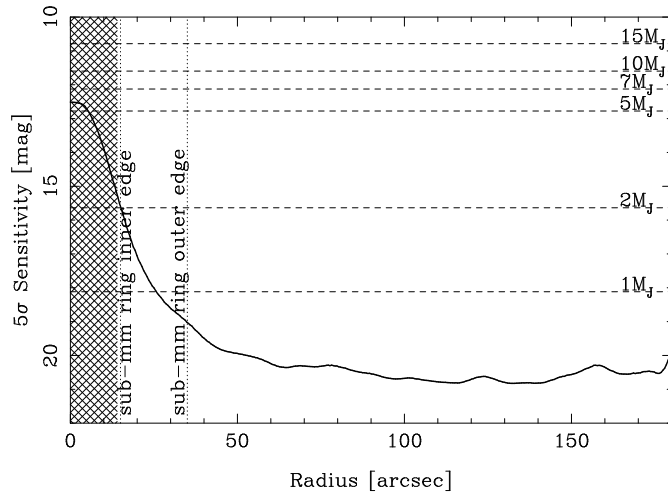
FIGURE 7. Residual noise, after PSF subtraction, of 4.5 μm ε Eridani radial profile (Marengo *et al.* [51]). Dashed lines are the predicted fluxes (from Burrows, Sudarsky, and Lunine [49]) of 1 Gyr old planets with mass from 1 to 15 M$_J$. Dotted lines enclose the region where the sub-millimeter debris disk around this star is located.

multiple new giant transiting planets (February 2009 launch). The observing cadence of the Kepler mission is not optimized for transit timing (Basri *et al.* [45]), so transit timing observations in the Kepler field by Warm Spitzer could leverage and enhance Kepler's science return.

8. DIRECT IMAGING

Although the bulk of Spitzer's results for exoplanets have relied on time series photometry and spectroscopy, Spitzer's high sensitivity in imaging mode is also important for exoplanet imaging studies. Radial velocity surveys have reached the precision required to detect planets only in the last 10 years, so little is known about the frequency of exoplanets and other low mass companions at distances greater than $\sim$ 5 - 10 AU. This is unfortunate because determining the presence of planetary mass bodies in the periphery of known exoplanetary systems has important implications for their evolution. These include studying the dynamical "heating" of the orbits in the system, which may result in higher eccentricities (or even expulsion) of some components, or in enhanced collision rates between the bodies in extrasolar Kuiper belts, which may be responsible for the formation of transient debris disks.

Imaging can in principle fill this observational gap. Three objects of near planetary mass have already been detected within 300 AU from the primary around the brown dwarf 2M1207 (Chauvin *et al.* [46]) and the stars GQ Lup (Neuhauser *et al.* [47]) and AB Pic (Chauvin *et al.* [48]) with ground based adaptive optics observations. Other optical and near-IR searches from the ground and from space, have so far produced negative results.

Warm Spitzer may provide a significant contribution in this arena, as the two surviving IRAC bands are particularly suited for the detection of cool extrasolar planets and brown

dwarf companions (T and the so-called Y dwarfs). A gap in molecular opacities of giant planets near 4.5 μm allows emission from deep, warmer atmospheric layers to escape: giant planets are very bright at this wavelength (Burrows, Sudarsky, and Lunine [49]). A strong methane absorption band strongly depresses the planetary flux at 3.6 μm: as a result, the IRAC [3.6]-[4.5] color of planetary mass bodies is expected to be unique, and allow for their identification among background objects in the field. Model atmosphere calculations predict that a 1 Gyr old, 2 M$_J$ planet around a star 10 pc from the Sun will have a 4.5 μm magnitude of $\sim$ 18. Such planets are detectable today with IRAC provided that the diffracted light from the central bright star can be removed at the planet's image location. The stability of Spitzer's optical and pointing systems assures that the stellar Point Spread Function (PSF) is highly reproducible, allowing much fainter nearby sources to be identified in the PSF wings using differential measurements.

This search has already been carried out for the debris disk star ε Eridani, which is also home of a Jovian class radial velocity planet orbiting the star at 3.4 AU (Hatzes *et al.* [50]). The search has set stringent limits for the mass of external planetary bodies in the system (including the area occupied by the debris disk, Marengo *et al.* [51]), and demonstrated that this technique is sensitive to the detection of planets with mass as low as 1 M$_J$ (Fig. 7) outside the 14 arcsec radius (50 AU) where the IRAC frames are saturated. The search radius can be reduced to $\sim$ 5 arcsec or less by using shorter frame times available in IRAC subarray mode. A pilot search of 16 nearby stellar systems is being conducted in Spitzer cycles 3 and 4. These programs will identify possible candidates based on their [3.6]-[4.5] colors, which will need to be verified by second epoch observations during the warm mission, to detect their common proper motion with the primary.

The Spitzer warm mission will provide the opportunity to extend the search of planetary mass companions through imaging techniques to a large number of systems in the solar neighborhood, probing a search radius from $\sim$ 10 to 10,000 AU around stars within 30 pc from the Sun. This search will be sensitive to masses as low as a few Jupiter masses, depending on the age and distance of the systems. These observations will be complementary to ground based radial velocity and imaging searches with adaptive optics systems, given the larger field of view and higher sensitivity of IRAC, in a wavelength range where the required contrast ratio (as low as 10^{-5} of the parent star flux) is more accessible than in the optical and near-IR.

ACKNOWLEDGMENTS

REFERENCES

1. Werner, M. W., *et al.*, 2004, ApJS, 154, 1.
2. Charbonneau, D., *et al.*, 2005, ApJ, 626, 523.
3. Deming, D. *et al.*, 2005, Nature, 434, 740.
4. Knutson, H., *et al.*, 2007a, Nature, 447, 183.
5. Grillmair, C. *et al.*, 2007, ApJ 658, L115.
6. Richardson, L. J. *et al.*, 2007, Nature 445, 892.
7. Fischer, D., *et al.*, 2005, ApJ 620, 481.
8. Burke, C., *et al.*, 2007, submitted to ApJ, (astro-ph/0705.0003).
9. O'Donovan, F. T., *et al.*, 2007, ApJ 663, L37.
10. Johns-Krull, C., *et al.*, 2007, BAAS 39, 096.05.
11. Mandushev, G., *et al.*, 2007, ApJ, in press, (astro-ph/0708.0834).
12. Torres, G., *et al.*, 2007, ApJ, 666, L121.
13. Gillon, M., *et al.*, 2007a, A&A, 472, L13.
14. Butler, R. P., *et al.*, 2004, ApJ 617, 580.
15. Johnson, J. A., *et al.*, 2007, ApJ, 655, 785
16. Richardson, L. J. *et al.*, 2006, ApJ 649, 1043.
17. Charbonneau, D., *et al.*, 2006, ApJ 636, 445.
18. Sato, B., *et al.*, 2005, ApJ 633, 465.
19. Lissauer, J. J. and Stevenson, D. J., 2007, in Protostars and Planets V, (editors D. Jewitt and B. Reipurth), 591.
20. Bodenheimer, P., Laughlin, G., and Lin, D. N. C. 2003, ApJ 592, 555.
21. Winn, J. N., *et al.*, 2007, AJ 133, 1828.
22. Deming, D., *et al.*, 2007a, ApJL, in press, (astro-ph/0707.2778).
23. Gillon, M., *et al.*, 2007b, A&A 471, L51.
24. Reach, W. T., *et al.*, 2005, PASP 117, 978.
25. Knutson, H., *et al.*, ApJ, submitted.
26. Charbonneau, D., *et al.*, 2007, in Protostars and Planets V, (editors D. Jewitt and B. Reipurth), 701.
27. Thommes, E. W., 2005, ApJ 626, 1033.
28. Seager, S., *et al.*, 2007, ApJ, in press (astro-ph/0707.2895).
29. Rivera, E. J., *et al.*, 2005, ApJ 634, 625.
30. Snellen, I. A. G., and Covino, E., 2006, MNRAS 375, 307.
31. Deming, D. *et al.*, 2007, MNRAS, 378, 148.
32. Burrows, A. *et al.*, ApJL, in press.
33. Cooper, C. S., & Showman, A. P. 2005, ApJ, 629, L45.
34. Rauscher, E., *et al.*, 2007, ApJ, 662, L115.
35. Cowan, N. B., Agol, E., and Charbonneau, D., 2007, MNRAS, 379, 641.
36. Naef, D., *et al.*, 2001, A&A 375, L27.
37. Langton, J., and Laughlin, G., 2007, ApJ 657, L113.
38. Johnson, J. A., *et al.*, 2006, ApJ 652, 1724.
39. Williams, P. K. G., *et al.*, 2006, ApJ 649, 1020.
40. Agol, E., *et al.*, 2005, MNRAS 359, 567.
41. Holman, M. J., and Murray, N. M., 2005, Science 307, 1288.
42. Steffen, J., and Agol, E., 2005, MNRAS 364, L96.
43. Agol, E., and Steffen, J., 2007, MNRAS 374, 941.
44. Pont, F., *et al.*, 2007, A&A, submitted (astro-ph/0707.1940).
45. Basri, G., Borucki, W. J., and Koch, D. 2005, New Astron. Rev. 49, 478.
46. Chauvin, G. *et al.*, 2004, A&A 425, L29.
47. Neuhauser, R. *et al.*, 2005, A&A 345, L13.
48. Chauvin, G. *et al.*, 2005, A&A 438, L29.
49. Burrows, A., Sudarsky, D., and Lunine, J. L. 2003, ApJ 596, 587.
50. Hatzes, A. P. *et al.*, 2000, ApJ 544, L145.
51. Marengo, M. *et al.*, 2006, ApJ 647, 1437.